

Alma Mater Studiorum Università di Bologna
Archivio istituzionale della ricerca

Improved centrifugal and hyperfine analysis of ND₂H and NH₂D and its application to the spectral line survey of L1544

This is the final peer-reviewed author's accepted manuscript (postprint) of the following publication:

Published Version:

Improved centrifugal and hyperfine analysis of ND₂H and NH₂D and its application to the spectral line survey of L1544 / Melosso M.; Bizzocchi L.; Dore L.; Kisiel Z.; Jiang N.; Spezzano S.; Caselli P.; Gauss J.; Puzzarini C.. - In: JOURNAL OF MOLECULAR SPECTROSCOPY. - ISSN 0022-2852. - STAMPA. - 377:(2021), pp. 111431.111431-1-111431.111431-8. [10.1016/j.jms.2021.111431]

Availability:

This version is available at: <https://hdl.handle.net/11585/867650> since: 2022-02-24

Published:

DOI: <http://doi.org/10.1016/j.jms.2021.111431>

Terms of use:

Some rights reserved. The terms and conditions for the reuse of this version of the manuscript are specified in the publishing policy. For all terms of use and more information see the publisher's website.

This item was downloaded from IRIS Università di Bologna (<https://cris.unibo.it/>).
When citing, please refer to the published version.

(Article begins on next page)

This is the final peer-reviewed accepted manuscript of:

M. Melosso, L. Bizzocchi, L. Dore, Z. Kisiel, N. Jiang, S. Spezzano, P. Caselli, J. Gauss, C. Puzzarini. Improved centrifugal and hyperfine analysis of ND₂H and NH₂D and its application to the spectral line survey of L1544. J. Mol. Spectrosc. 377 (2021) 111431

The final published version is available online at:

<https://doi.org/10.1016/j.jms.2021.111431>

Terms of use:

Some rights reserved. The terms and conditions for the reuse of this version of the manuscript are specified in the publishing policy. For all terms of use and more information see the publisher's website.

This item was downloaded from IRIS Università di Bologna (<https://cris.unibo.it/>)

When citing, please refer to the published version.

Improved centrifugal and hyperfine analysis of ND₂H and NH₂D and its application to the spectral line survey of L1544

Mattia Melosso^{a,*}, Luca Bizzocchi^b, Luca Dore^a, Zbigniew Kisiel^c, Ningjing Jiang^a, Silvia Spezzano^b, Paola Caselli^b, Jürgen Gauss^d, Cristina Puzzarini^{a,*}

^a*Dipartimento di Chimica “Giacomo Ciamician”, Università di Bologna, Via F. Selmi 2, 40126 Bologna, Italy*

^b*Center for Astrochemical Studies, Max Planck Institut für extraterrestrische Physik, Gießenbachstraße 1, 85748 Garching bei München, Germany*

^c*Institute of Physics, Polish Academy of Sciences, Al. Lotników 32/46, 02-668 Warszawa, Poland*

^d*Department Chemie, Johannes Gutenberg-Universität Mainz, Duesbergweg 10-14, 55128 Mainz, Germany*

Abstract

Quantifying molecular abundances of astrochemical species is a key step towards the understanding of the chemistry occurring in the interstellar medium. This process requires a profound knowledge of the molecular energy levels, including their structure resulting from weak interactions between nuclear spins and the molecular rotation. With the aim of increasing the quality of spectral line catalogs for the singly- and doubly-deuterated ammonia (NH₂D and ND₂H), we have revised their rotational spectra by observing many hyperfine-resolved lines and more accurate high-frequency transitions. The measurements have been performed in the submillimeter-wave region (265–1565 GHz) using a frequency modulation submillimeter spectrometer and in the far-infrared domain (45–220 cm⁻¹) with a synchrotron-based Fourier-transform interferometer. The analysis of the new data, with the interpretation of the hyperfine structure supported by state-of-the-art quantum-chemical calculations, led to an overall improvement of all spectroscopic parameters. Moreover, the effect of the inclusion of deuterium splittings in the analysis of astrophysical NH₂D emissions at millimeter wavelengths has been tested using recent observations of the starless core L1544, an ideal astrophysical laboratory for the study of deuterated species. Our results show that accounting for hyperfine interactions leads to a small but significant change in the physical parameters used to model NH₂D line emissions.

Keywords: Ammonia, Hyperfine structure, Rotational spectroscopy, Interstellar medium, Deuterium fractionation, Starless core

1. Introduction

The increasing sensitivity and spectral resolution of modern radio-telescopes are stimulating a large number of laboratory studies that aim at supporting astronomical observations of molecules in the Interstellar Medium (ISM). On the one hand, these studies mostly exploit rotational spectroscopy techniques to characterize small- to medium-sized species, the reason being that rotational signatures can undoubtedly prove (and quantify) the presence

of a molecule in the ISM [1]. On the other hand, laboratory efforts on a particular molecular system can be motivated by several aspects. Among them, the search for pre-biotic species and molecules that are more generally related to the origin of life is still one of the hottest topics in astrochemistry [2, 3, 4], although any attempt to detect amino acids in the gas-phase has so far remained unsuccessful [5, 6]. However, being evident that the ISM exhibits a complex chemistry, the characterization of new Complex Organic Molecules (COMs, i.e. species containing at least six atoms and composed of carbon, hydrogen, oxygen and/or nitrogen) is the main theme of joint laboratory-observational studies [7, 8, 9, 10]. Moreover, the new detections of

*Corresponding authors

Email addresses: mattia.melosso2@unibo.it (Mattia Melosso), cristina.puzzarini@unibo.it (Cristina Puzzarini)

ions [11], radicals [12], carbon-chains [13, 14], and rings [15] –including aromatic ones [16]– open new perspectives for an even richer molecular complexity.

All these aspects contribute to our understanding of the interstellar chemistry and are useful to probe excitation mechanisms and kinematics, as well as to trace the evolutionary stage of astronomical objects [17, 18] and their chemical differentiation [19, 20, 21]. However, the evaluation of molecular abundances, which are in turn the building-blocks of astrochemical models, is a crucial point that requires a deep knowledge of the molecule under investigation: this can include information about vibrational excited states [22, 23], a correct computation of partition function values [24], or the effect of nuclear electric and magnetic interactions giving raise to the so-called hyperfine structures (HFS).

Recently, the importance of such effects in the analysis of singly-deuterated ammonia (NH₂D) line emission towards the starless core H-MM1 has been pointed out [25, 26] and, subsequently, addressed in our laboratory in Bologna [27]. In the context of a broader investigation of the rotational spectra of ammonia isotopologues, we have extended the centrifugal analysis of NH₂D and ND₂H at higher frequencies and measured additional hyperfine-resolved transitions, especially those of astronomical interest. The new measurements have been combined with literature data to obtain the best set of spectroscopic constants for both singly- and doubly-deuterated ammonia, in order to generate accurate line catalogs. Then, the effect of including deuterium hyperfine interactions on the analysis of astrophysical NH₂D emissions at millimeter wavelengths has been tested using recent observations of the low-mass star-forming core L1544.

The paper is organized as follows. First, the spectral features of the rotation-inversion spectrum of ND₂H compared to that of NH₂D (Section 2) are presented. Then, the submillimeter spectrometer and the synchrotron-based Fourier transform interferometer used for the measurements are described (Section 3). In Section 4, the results of our spectral analysis are given and applied to NH₂D line emissions towards the starless core L1544. Finally, our findings are summarized in Section 5.

2. Theory

The main features of the rotational spectrum of NH₂D have been exhaustively described in Melosso *et al.* ([27], hereafter **Paper I**). The spectroscopic behavior of ND₂H is quite similar to that of NH₂D; therefore, we only briefly recall the key aspects and highlight the major differences.

Doubly-deuterated ammonia is an asymmetric-top rotor with a double-minima potential energy surface. The tunneling between the two equivalent configurations splits each J_{K_a, K_c} rotational level into two sub-levels, one symmetric (*s*) and one anti-symmetric (*a*) with respect to inversion. As in the case of NH₂D, the inversion motion of ND₂H occurs along the *c*-axis; however, the *a*- and *b*-axes are reversed. Hence, the spectrum of ND₂H is characterized by weak *b*-type transitions within each sub-state and stronger *c*-type transitions connecting the two inversion states [28].

All nuclei present in the molecule having nonzero nuclear spins contribute to the hyperfine structure of the rotational spectrum of ND₂H. The HFS is dominated by the nuclear quadrupole coupling (NQC) of nitrogen, but spin-rotation (SR) interactions as well as NQC effects due to the deuterium nuclei have an appreciable impact on it. Moreover, the presence of two equivalent D nuclei leads to the existence of *ortho* and *para* species, and the total nuclear spin $I_{D, \text{tot}} = I_{D_1} + I_{D_2}$ must be taken into account. The *ortho* species corresponds to $I_{D, \text{tot}} = 0$ or 2, whereas the *para* form is characterized by $I_{D, \text{tot}} = 1$. This results in an *ortho:para* spin-statistical weight ratio of 2:1. Since the two equivalent particles are bosons, the Bose-Einstein statistics holds. Given that the total wavefunction has to be symmetric with the respect to the exchange of the two D nuclei, the *ortho* form has rotation-inversion states of the type (*s, ee*), (*s, oo*), (*a, eo*), and (*a, oe*), while the *para* species possesses (*s, eo*), (*s, oe*), (*a, ee*), and (*a, oo*) states.

While the Hamiltonian used in the present analysis is identical to the one described in **Paper I**, the angular momentum coupling scheme adopted for the labelling of energy levels is slightly different:

$$\begin{aligned} \mathbf{F}_1 &= \mathbf{J} + \mathbf{I}_N, \\ \mathbf{F}_2 &= \mathbf{F}_1 + \mathbf{I}_{D, \text{tot}}, \\ \mathbf{F} &= \mathbf{F}_2 + \mathbf{I}_H, \end{aligned} \quad (1)$$

because of the presence of the two identical deuterium nuclei and only one hydrogen.

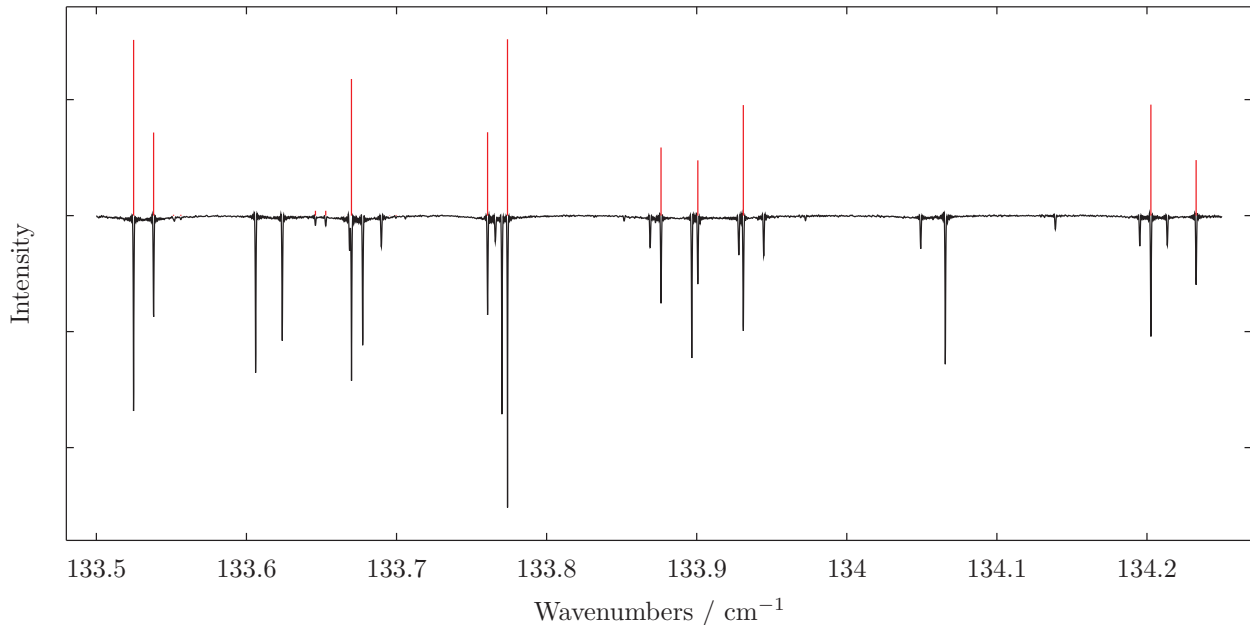


Figure 1: Portion of the FIR spectrum of ND_2H (black trace). The red bars indicate the position and intensity of some c -type R branch transitions, as predicted using the spectroscopic constants determined in this work. The remaining spectral lines belong to ND_3 or to other by-products of the discharge. The intensity on the y -axis is expressed in arbitrary units.

3. Experiment

Rotational transitions of singly- and doubly-deuterated ammonia were recorded in the range 265–1565 GHz with a frequency-modulation sub-millimeter spectrometer [29]. The radiation source of the spectrometer is constituted by a series of Gunn diodes emitting between 80 and 134 GHz, which can be coupled with passive frequency multipliers (doublers and triplers). Terahertz frequencies are obtained by connecting two triplers in cascade guided by Gunn diodes working in the F band (115–134 GHz) [30, 31]. However, the twelfth harmonic of their radiation remains detectable with a power around few tens of μW , thus enabling to reach frequencies up to 1.6 THz. The radiation source is phase-locked to a harmonic of a centimeter-wave synthesizer (2–18 GHz), frequency modulated at $f = 1 - 48$ kHz, and referenced to a 5 MHz rubidium atomic clock. The measurements were performed in a 3 m long glass absorption cell with the optical elements of the spectrometer arranged to perform, whenever possible, Lamb-dip measurements (for further details about the set-up, see **Paper I** as well as Refs. [32, 33, 34]). The output radiation was then detected by a liquid helium-cooled InSb bolometer and sent to a lock-in amplifier, set at twice the modulation frequency ($2f$

detection scheme). Here, the sample of NH_2D was produced using the same methodology employed in **Paper I** (a small flow of NH_3 in a cell where D_2 had been previously discharged), whereas a good yield of ND_2H was obtained by flowing simply ND_3 into the absorption cell.

Additional transitions in the range 45–220 cm^{-1} were observed at the SOLEIL synchrotron using a Bruker IFS125HR FTIR interferometer, whose source is the bright synchrotron radiation extracted by the AILES beamline. The far-infrared (FIR) spectrum was recorded at a resolution of 0.001 cm^{-1} , using the same set-up described in detail in Refs. [35, 36], during a measurement campaign of the ND_2 radical. Although the experimental conditions were not optimized to form deuterated isotopologues of ammonia, the use of ND_3 as precursor in a radio-frequency discharge produced strong –but not saturating– lines of ND_2H in the spectrum, as can be seen in Figure 1. Conversely, NH_2D seems to be much less abundant and only a few absorption lines were detected; therefore, its FIR spectrum could not be analyzed.

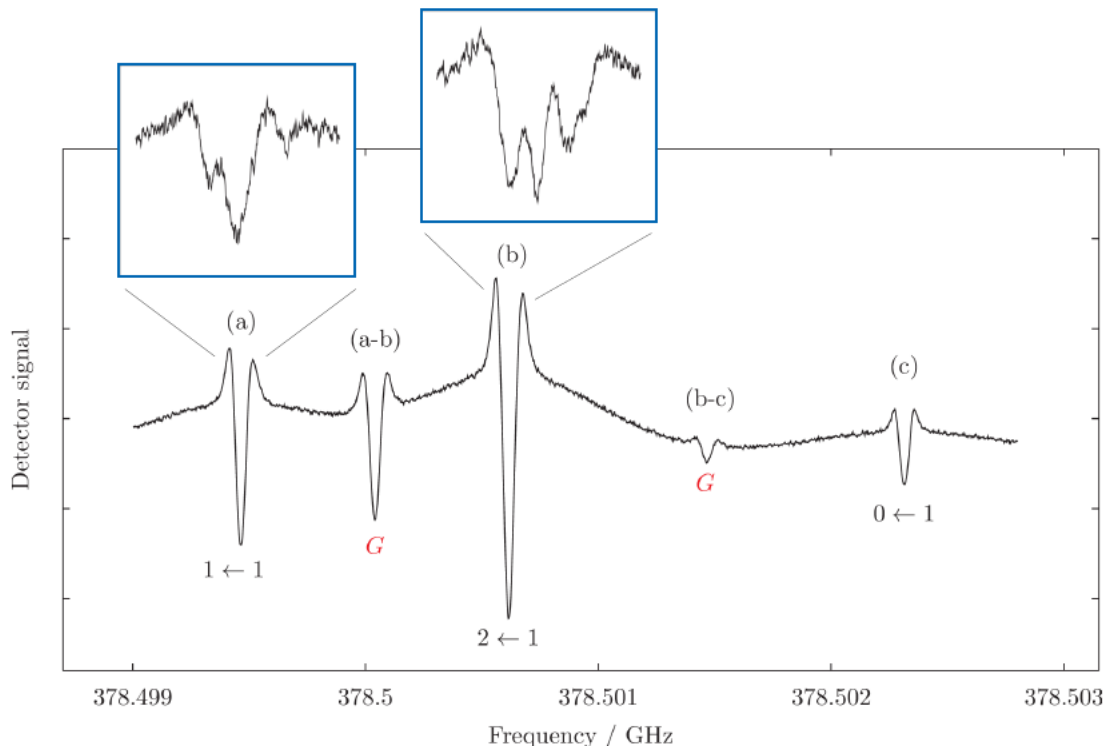


Figure 2: Lamb-dip spectrum of the $J_{K_a, K_c} = 1_{1,0}^{(s)} - 0_{0,0}^{(a)}$ p -ND₂H transition. The numbers below each HFS components refer to the $F_1' \leftarrow F_1$ quantum numbers, while a red G indicates a ghost feature. The labels above each line are used to denote the “interacting” transition frequencies from which the ghost transitions arise. The magnified boxes show the splittings due to deuterium quadrupolar interaction, as observed at higher-resolution experimental conditions. The vertical scale of the plots represents the detector response in arbitrary units.

4. Results

4.1. Spectral analysis

The latest sets of spectroscopic constants for NH₂D and ND₂H were retrieved from Paper I and the Cologne Database for Molecular Spectroscopy (CDMS) [37], respectively. The quality of these parameters was sufficient to search and assign rotational transitions from the submillimeter-wave (submm) to the far-infrared domain. Moreover, in order to correctly interpret the hyperfine structure of the ND₂H spectrum, the NQC, SR, and dipolar spin-spin (SS) tensors of doubly-deuterated ammonia were computed using the approach described in Paper I.

Briefly, the equilibrium values of the hyperfine constants were computed using the CCSD(T) method [38] in conjunction with a series of correlation-consistent n -uple-zeta basis sets [39, 40, 41, 42, 43] (with $n = Q, 5, 6$), correlating all electrons, and extrapolated to the complete basis set (CBS) limit. Then, exploiting the additiv-

ity approximation [44], the contributions due to the full treatment of triple and quadruple excitations were also taken into account using triple- and double-zeta basis sets, respectively. Subsequently, the equilibrium hyperfine parameters were augmented by the corresponding vibrational corrections in order to estimate the vibrational ground-state values. These corrections have been evaluated within the second-order vibrational perturbation theory (VPT2) [45] at the CCSD(T)/aug-cc-pCVQZ level of theory (with all electrons correlated). All CCSD(T) computations have been performed using the CFOUR package [46, 47], while the MRCC program [48, 49] interfaced to CFOUR has been employed for CCSDT and CCSDTQ calculations. The computed values of all NQC, SR, and SS interaction constants are listed in Table 1. According to the literature on this topic (see, e.g., Refs. [27, 32, 50]), the computational methodology employed is able to provide quantitative predictions of hyperfine parameters. In more detail, for nuclear

209 quadrupole coupling constants, the discrepancy be- 222
 210 tween experimental and computed values is below 223
 211 20 kHz for parameters as small as those encountered 224
 212 in this work. Moving to nuclear spin-rotation con- 225
 213 stants, discrepancies usually range from hundredths 226
 214 of kHz to a few kHz.

Table 1: Computed nuclear quadrupole, spin-rotation, and dipolar spin-spin coupling constants of ND₂H.

Constant	Atom	Unit	ND ₂ H
χ_{aa}	(N)	MHz	-2.048
χ_{cc}	(N)	MHz	-3.842
C_{aa}	(N)	kHz	5.229
C_{bb}	(N)	kHz	3.756
C_{cc}	(N)	kHz	4.000
χ_{aa}	(D)	MHz	0.135
χ_{cc}	(D)	MHz	-0.124
C_{aa}	(D)	kHz	-1.228
C_{bb}	(D)	kHz	-1.888
C_{cc}	(D)	kHz	-1.860
C_{aa}	(H)	kHz	-23.595
C_{bb}	(H)	kHz	-5.058
C_{cc}	(H)	kHz	-9.115
D_{bb}	(N-D)	kHz	0.19
D_{cc}	(N-D)	kHz	0.98
D_{bb}	(N-H)	kHz	-8.62
D_{cc}	(N-H)	kHz	0.66
D_{bb}	(H-D)	kHz	-4.89
D_{cc}	(H-D)	kHz	3.82
D_{bb}	(D-D)	kHz	0.65
D_{cc}	(D-D)	kHz	0.65

Notes: The nuclear quadrupole (χ_{ii}) and dipolar spin-spin coupling (D_{ii}) tensors have zero trace; therefore, only two of the three diagonal components are given.

215 For the first time, the complex hyperfine 261
 216 structure caused by the nitrogen and deuterium 262
 217 quadrupole couplings has been revealed in some low 263
 218 J transitions of ND₂H. As an example, Figure 2 264
 219 shows the Lamb-dip spectrum of the fundamen- 265
 220 tal c -type rotation-inversion transition $J_{K_a, K_c} =$ 266
 221 $1_{1,0}^{(s)} - 0_{0,0}^{(a)}$ of the *para* species. The main panel illus-

222 trates the three F_1 components ($\Delta F_1 = 0, \pm 1$) and 223
 224 two ghost transitions¹ (marked with a red G) oc- 225
 226 ccurring in between, while the magnified boxes high- 227
 228 light the deuterium HF splittings corresponding to 229
 230 different $F'_2 - F_2$ components. A similar resolution 231
 232 has been obtained also for the $J_{K_a, K_c} = 1_{1,0}^{(a)} - 0_{0,0}^{(s)}$ 233
 234 transition of *o*-ND₂H.

235 Additional measurements of NH₂D and ND₂H 236
 237 were performed with three main aims: (i) to re- 238
 239 solve the HFS as much as possible for those tran- 240
 241 sitions which can be used in astronomical observa- 242
 243 tions (typically involving low-energy levels), (ii) to 244
 245 exploit the Lamb-dip technique at THz frequencies 246
 247 in order to achieve an accuracy of about 10 ppb 248
 249 on the line position, and (iii) to revise the submm 249
 250 and FIR spectra at higher resolution. In particu- 251
 252 lar, we have observed about one hundred transi- 253
 254 tions of NH₂D and ND₂H in the mm/submm re- 255
 256 gion, half of which show the HFS at least partially 256
 257 resolved. For ND₂H only, we also detected and an- 257
 258 alyzed more than 700 distinct FIR transitions in- 258
 259 volving rotation-inversion levels with J up to 18.

260 The newly measured data were collected together 261
 262 with all pure-rotational literature data [51, 52, 53, 262
 263 54, 55, 28, 27] and processed into a combined anal- 263
 264 ysis. A least-squares procedure was performed 264
 265 with the SPFIT subroutine of the CALPGM program 265
 266 suite [56], where each datum is weighted propor- 266
 267 tionally to the inverse square of its uncertainty. 267
 268 The error associated to our line positions is in the 268
 269 range 2–100 kHz for mm/submm transitions and 269
 270 $5 \times 10^{-5} \text{ cm}^{-1}$ for FIR lines, while literature data 270
 271 were used with their declared uncertainty. **Unre-** 271
 272 **solved lines were incorporated in the fit as intensity-** 272
 273 **weighted average of the individual components in-** 273
 274 **olved in the blended feature, as implemented in** 274
 275 **SPFIT.**

276 The fit results for NH₂D and ND₂H have sim- 276
 277 ilar quality, despite the different number of avail- 277
 278 able data. The overall fit standard deviation (σ) 278
 279 is close to 1 in both cases and the root-mean-square 279
 280 (rms) error is below 100 kHz for mm/submm data 280
 281 and around 0.0002 cm^{-1} for the FIR transitions. 281
 282 These values indicate that the modeling of both 282
 283 species is satisfactory and can be used to generate 283
 284 spectral predictions in a wide range of frequencies 284
 285

¹Ghost transitions, also denoted as crossover resonances, are due to the saturation of overlapping Gaussian profiles of two transitions sharing a common energy level. They occur at the arithmetic mean frequency of the overlapping transitions.

with a low uncertainty. The derived rotational and centrifugal distortion constants, Coriolis interaction terms, and HFS parameters are given in Tables 2–4. All parameters have been improved, with respect to previous studies, by up to one order of magnitude. Moreover, the ND₂H quadrupole coupling constant $\chi_{cc}(\text{D})$ has been determined for the first time and allows the simulation of the deuterium HFS. **Its derived value, -0.121(4), agrees very well with the computed counterpart, -0.124. Instead, the hydrogen HFS could not be resolved in the laboratory spectra, thus preventing the experimental determination of the hydrogen spin-rotation constants. Simulations based on the calculated parameters showed that the hydrogen HFS is so small that it does not affect the spectral linewidths.**

The SPFIT input files (.PAR and .LIN) as well as a re-formatted version of the .FIT output file are provided for both species as Supplementary Material.

4.2. Line catalogs for astronomical purposes

In order to produce meaningful line lists that can be used for astronomical observations of NH₂D and ND₂H, the new sets of spectroscopic constants must be combined with accurate estimates of the rotational partition function (Q_{rot}) and dipole moment components. The latter were evaluated in Refs. [54] and [28] and are: $\mu_a = -0.185$ D and $\mu_c = 1.46$ D for NH₂D and $\mu_b = 0.21$ D and $\mu_c = 1.47$ D for ND₂H.

The rotational partition functions, instead, have been calculated numerically using the SPCAT subroutine of the CALPGM suite [56]. The temperature dependence of Q_{rot} was computed separately for the *ortho* and *para* species at three different “resolutions”: (i) without the inclusion of any HFS, (ii) considering only the contribution of nitrogen, and (iii) including the effects of both N and D nuclei. **These distinctions have been made in order to support the analysis of interstellar deuterated ammonia at different spectral resolution. Moreover, at the low temperatures of cold molecular clouds (5–10 K), the *ortho* and *para* species must be treated as separate species.** The rotational partition function values computed at temperatures between 2.725 and 300 K are provided as Supplementary Material.

4.3. Application to L1544 starless core spectrum

To test the effect of the inclusion of D hyperfine structure in the analysis of astrophysical NH₂D

Table 2: Ground-state rotational and centrifugal distortion constants up to the sixth power of the angular momentum.

Constant ^(a)	Unit	NH ₂ D	ND ₂ H
ΔE	MHz	12169.466(1)	5118.8865(8)
A	MHz	290074.6(2)	223187.715(1)
ΔA	MHz	-46.9120(8)	-16.1290(6)
B	MHz	192176.4768(8)	160214.998(4)
ΔB	MHz	-17.34(2)	-5.3284(4)
C	MHz	140810.2(2)	112520.741(4)
ΔC	MHz	11.2003(1)	4.0868(4)
D_J	MHz	15.7199(1)	3.5183(2)
ΔD_J	MHz	-0.09412(4)	-0.000896(5)
D_{JK}	MHz	-23.7516(2)	-2.9356(9)
ΔD_{JK}	MHz	0.19484(9)	-0.01008(3)
D_K	MHz	10.8484(3)	19.2808(7)
ΔD_K	MHz	-0.10982(6)	-0.04472(5)
d_1	MHz	4.14089(8)	-1.2318(2)
Δd_1	MHz	-0.04166(4)	0.000795(4)
d_2	MHz	0.13787(4)	-0.28029(7)
Δd_2	MHz	0.00567(3)	0.001787(2)
H_J	kHz	3.537(3)	0.3353(9)
ΔH_J	kHz	-0.1940(5)	0.00160(5)
H_{JK}	kHz	-8.422(4)	-1.21(1)
ΔH_{JK}	kHz	0.4048(8)	-0.0055(2)
H_{KJ}	kHz	8.776(7)	2.16(4)
ΔH_{KJ}	kHz	-0.3824(9)	-0.049(1)
H_K	kHz	-3.705(8)	4.75(3)
ΔH_K	kHz	0.1762(4)	-0.089(1)
h_1	kHz	-1.832(3)	0.247(1)
Δh_1	kHz	0.1097(6)	-0.00060(3)
h_2	kHz	0.445(2)	0.0382(5)
Δh_2	kHz	-0.0146(6)	-0.00160(2)
h_3	kHz	-0.0403(5)	0.0225(2)
Δh_3	Hz	-0.0086(3)	-0.00097(1)

Notes: Numbers in parentheses are standard errors and apply to the last significant digits. ^(a) For a given parameter X , $\Delta X = (X^{(a)} - X^{(s)})/2$.

emissions at millimeter wavelengths, we have used recent observations of the starless core L1544, a low-mass star-forming core in a very early stage of evolution. This source is a prototypical cold, quiescent core on the verge of the gravitational collapse, which exhibits very narrow line emissions due its low central temperature, subsonic contraction motion, and low turbulence [57, 58]. It also shows a high degree of deuteration [e.g., Ref. 59]) which

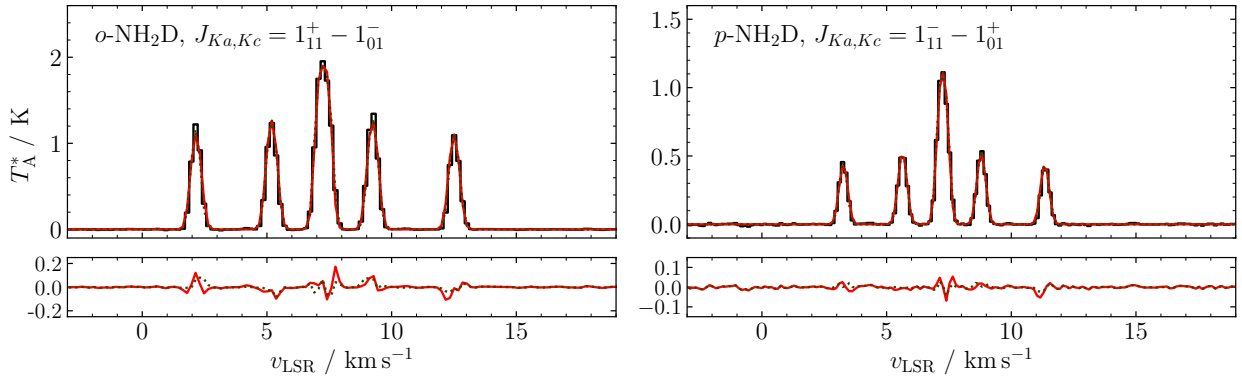


Figure 3: Spectra of the NH₂D transitions observed towards L1544. (*Top left panel*): $J_{K_a, K_c} = 1_{1,1}^{(s)} - 1_{0,1}^{(a)}$ *ortho* line at 85926.3 MHz. (*Top right panel*): $J_{K_a, K_c} = 1_{1,1}^{(a)} - 1_{0,1}^{(s)}$ *para* line at 110153.6 MHz. The dotted green trace plots the model computed considering the full HFS (N+D). The solid red trace plots the model computed with the N quadrupole only. (*Bottom panels*): Residuals of both models, plotted using the same colour legend.

326 makes it an ideal astrophysical laboratory to observe D-containing molecules and to reveal subtle spectral effects due to the contribution of the deuterium quadrupole splittings.

327
328
329
330 The astronomical data used here were collected using the IRAM 30m telescope (Pico Veleta, Spain) in the past few years by some members of our team. They were observed as part of the projects 008-12, 013-13 (PI S. Spezzano) and 150-11, 127-12 (PI L. Bizzocchi). The observing runs were performed in several sessions from May 2012 to October 2013. The frequency intervals of interest have been extracted from the output of the wide-band FTS spectrometer which was connected to the 3 mm band of the EMIR heterodyne receiver. The *o*-NH₂D lines at 85926.3 MHz and the ones of *p*-NH₂D at 110153.6 MHz were observed in the lower-outer (LO) and upper-inner (UI) sub-band, respectively. A detailed description of the observation strategy and the data reduction can be found elsewhere [60, 61, 62].

347 The resulting spectra are shown in the two panels of Figure 3, plotted as black histograms. Note that the *x*-axis is labelled in radial equivalent velocity using the rest frequency of the corresponding unsplit lines as reference. The solid red lines plot the best fit model computed using the full HFS (including D). The fitting was performed using a custom Python3 code described in Ref. [12]. The free parameters of the optimisation are the column density (N), the excitation temperature (T_{ex}), the systemic velocity (v_{LSR}) and the line full-width-half-maximum (FWHM), while the total opacity of the

359 transition (τ) is regarded as a derived quantity.

360 Table 5 collects the fit results of two different analyses obtained by taking into account the nitrogen quadrupole coupling only (column labelled by N) or the full hyperfine structure including the deuterium effects (N+D). While the two models would be virtually indistinguishable by visual inspection, small but significant differences are highlighted by the fit results. Apart from a 30-40% reduction of the residual rms, the proper treatment of the hyperfine effects entails a reduction of the derived line FWHM of about 12%. This change is reflected by the values of the related parameter N and T_{ex} , and of the derived quantity τ . For the less opaque emission (*p*-NH₂D), the column density and the excitation temperature readjust, while τ remains substantially unchanged. For the thicker *o*-NH₂D line, the T_{ex} is unaffected and the deviation is mainly observed by a relevant change of τ .

378 5. Conclusions

379 The rotational spectra of singly- and doubly-deuterated ammonia have been thoroughly re-investigated at higher resolution. By means of the Lamb-dip technique at submillimeter wavelengths and with the use of synchrotron radiation in the FIR region, a large number of transitions have been measured with high accuracy. For some of them, the nitrogen and deuterium hyperfine structure due to electric and magnetic interactions has been unveiled, thus allowing the precise determination of

Table 3: Higher-order centrifugal distortion constants and Coriolis interaction parameters.

Constant ^(a)	Unit	NH ₂ D	ND ₂ H
L_J	Hz	-1.14(2)	
ΔL_J	mHz	181.(2)	-3.7(1)
L_{JJK}	Hz	3.27(2)	-0.123(5)
ΔL_{JJK}	Hz	-0.468(5)	
L_{JK}	Hz	-5.63(7)	-0.50(4)
ΔL_{JK}	Hz	0.711(8)	
L_{KKJ}	Hz	5.1(1)	1.4(1)
ΔL_{KKJ}	Hz	-0.729(6)	0.30(1)
L_K	Hz	-2.1(1)	-3.60(6)
ΔL_K	Hz	0.306(2)	-0.026(6)
l_1	Hz	0.80(2)	0.080(3)
Δl_1	mHz	-22.(2)	0.38(5)
l_2	Hz	-0.30(1)	-0.0185(3)
Δl_2	mHz	-152.(6)	1.98(6)
l_3	mHz	18.(3)	-4.7(2)
Δl_3	mHz	112.(5)	0.14(5)
l_4	mHz		-1.55(6)
Δl_4	mHz	-22.(1)	0.48(1)
M_{KKJ}	mHz		1.35(3)
M_K	mHz	1.3(3)	1.35(3)
F_{ij}	MHz	-5097.(3)	3129.49(4)
F_{ij}^J	MHz		0.812(3)
F_{ij}^K	MHz		-9.00(2)
F_{ij}^{JJ}	kHz		-1.49(2)
F_{ij}^{JK}	kHz		4.4(1)
F_{ij}^{KK}	kHz		9.8(4)
F_{ij}^{JJJ}	Hz		-1.22(4)

Notes: Numbers in parentheses are standard errors and apply to the last significant digits. ^(a) For a given parameter X , $\Delta X = (X^{(a)} - X^{(s)})/2$. F_{ij} corresponds to F_{ab} and F_{bc} for NH₂D and ND₂H, respectively.

nuclear quadrupole coupling and spin-rotation constants. Moreover, all the values of rotational and centrifugal distortion parameters could be refined thanks to the analysis of an extended dataset.

The new set of spectroscopic constants has been then used to evaluate the impact of the deuterium HFS on the analysis of astrophysical NH₂D lines towards L1544. The narrow line emissions of this pre-stellar core made it possible to detect small but significant differences in the physical parameters determined when both nitrogen and deuterium hyperfine interactions are taken into account. In addition

Table 4: Nitrogen and deuterium hyperfine constants (only the parameters used in the analyses are listed).

Constant	Atom	Unit	NH ₂ D	ND ₂ H
χ_{aa}	(N)	MHz	1.909(3)	-2.038(8)
χ_{cc}	(N)	MHz	-3.948(1)	-3.852(2)
C_{aa}	(N)	kHz	6.1(8)	5.229
C_{bb}	(N)	kHz	3.8(7)	3.756
C_{cc}	(N)	kHz	5.1(2)	4.000
χ_{aa}	(D)	MHz	0.225(5)	0.132
χ_{cc}	(D)	MHz	-0.135(1)	-0.121(4)
C_{aa}	(D)	kHz	-0.125	-1.228
C_{bb}	(D)	kHz	-3.154	-1.888
C_{cc}	(D)	kHz	-2.27(9)	-1.860

Notes: Numbers within parentheses are the standard errors and apply to the last significant digits. Non-determinable parameters (values given without error) have been kept fixed at the corresponding computed values (see Table 1).

to the improvement of the fit results in term of rms residual, the observed reduction of the line FWHM produces a change in the determination of the column density of *ortho*- and *para*-NH₂D of about 5–20 %. This observation demonstrates the importance of modelling all the effects that can contribute to the determination of molecular abundances for interstellar species.

6. Supplementary Material Available

The file “partition-function-values.pdf” contains the rotational partition function values computed at temperatures between 2.725 and 300 K for the *ortho* and *para* species of ND₂H and NH₂D. The files “nh2d.lin”, “nh2d.par”, “nd2h.lin”, and “nd2h.par” are the SPFIT input files used in our analysis. The files “nh2d_reformatted.out” and “nd2h_reformatted.out” are a reformatted version of the SPFIT output files.

7. Acknowledgement

This study was supported by Bologna University (RFO funds) and by MIUR (Project PRIN 2015: STARS in the CAOS, Grant Number 2015F59J3R), and in Mainz by the Deutsche Forschungsgemeinschaft via grant GA 370/6-2. Part of the measurements has been performed under the SOLEIL

Table 5: Analysis of the ortho and para NH₂D emissions in L1544 considering nitrogen quadrupole coupling only (N) or the full hyperfine structure (N+D).

Parameter	Unit	<i>o</i> -NH ₂ D		<i>p</i> -NH ₂ D	
		N	N+D	N	N+D
N	10 ¹⁴ cm ⁻²	5.92(20)	5.64(15)	3.01(14)	2.44(9)
T_{ex}	K	4.46(2)	4.47(2)	3.95(3)	4.07(2)
v_{LSR}	km s ⁻¹	7.265(2)	7.265(2)	7.194(1)	7.195(1)
FWHM	km s ⁻¹	0.444(3)	0.388(3)	0.389(3)	0.346(2)
τ^a		7.47	8.22	3.48	3.46
rms ^b	mK	56	39	19	11

Notes: Numbers within parentheses are the standard errors and apply to the last significant digits. ^a Derived quantity. ^b Root-mean-square of the residuals computed on lines.

426 proposal #20110017; we acknowledge the SOLEIL 462
 427 facility for provision of synchrotron radiation and 463
 428 would like to thank the AILES beamline staff for 464
 429 their assistance and in particular Dr. M.-A. Martin- 465
 430 Drumel and Dr. O. Pirali for their help during the 466
 431 spectral recording. L.B., S.S, and P.C. acknowl- 467
 432 edge the support by the Max Planck Society. N.J. 468
 433 thanks the China Scholarships Council (CSC) for 469
 434 the financial support. 470

435 References

436 [1] B. A. McGuire, 2018 Census of Interstellar, Circumstel- 477
 437 lar, Extragalactic, Protoplanetary Disk, and Exoplanetary 478
 438 Molecules, *Astrophys. J. Suppl. S.* 239 (2018) 17. 479
 439 [2] A. López-Sepulcre, N. Balucani, C. Ceccarelli, 480
 440 C. Codella, F. Dulieu, P. Theulé, Interstellar formamide 481
 441 (NH₂CHO), a key prebiotic precursor, *ACS Earth* 482
 442 *Space Chem.* 3 (10) (2019) 2122–2137. 483
 443 [3] V. M. Rivilla, J. Martín-Pintado, I. Jiménez-Serra, 484
 444 S. Martín, L. F. Rodríguez-Almeida, M. A. Requena- 485
 445 Torres, et al., Prebiotic precursors of the primordial 486
 446 RNA world in space: Detection of NH₂OH, *Astrophys.* 487
 447 *J. Lett.* 899 (2) (2020) L28. 488
 448 [4] S. A. Sandford, M. Nuevo, P. P. Bera, T. J. Lee, Pre- 489
 449 biotic astrochemistry and the formation of molecules of 490
 450 astrobiological interest in interstellar clouds and proto- 491
 451 stellar disks, *Chem. Rev.* 492
 452 [5] Y.-J. Kuan, S. B. Charnley, H.-C. Huang, W.-L. Tseng, 493
 453 Z. Kisiel, Interstellar glycine, *Astrophys. J.* 593 (2) 494
 454 (2003) 848. 495
 455 [6] L. E. Snyder, F. J. Lovas, J. M. Hollis, D. N. Friedel, 496
 456 P. R. Jewell, A. Remijan, et al., A rigorous attempt to 497
 457 verify interstellar glycine, *Astrophys. J.* 619 (2) (2005) 498
 458 914–930. doi:10.1086/426677. 499
 459 URL <https://doi.org/10.1086/426677> 500
 460 [7] M. Melosso, B. A. McGuire, F. Tamassia, C. Degli Es- 501
 461 posti, L. Dore, Astronomical search of vinyl alcohol as-

462 463
 464 465
 466 467
 468 469
 470 471
 472 473
 474 475
 476 477
 478 479
 480 481
 482 483
 484 485
 486 487
 488 489
 490 491
 492 493
 494 495
 496 497
 498 499
 500 501
 502 503
 504 505
 506 507
 508 509
 510 511
 512 513
 514 515
 516 517
 518 519
 520 521
 522 523
 524 525
 526 527
 528 529
 530 531
 532 533
 534 535
 536 537
 538 539
 540 541
 542 543
 544 545
 546 547
 548 549
 550 551
 552 553
 554 555
 556 557
 558 559
 560 561
 562 563
 564 565
 566 567
 568 569
 570 571
 572 573
 574 575
 576 577
 578 579
 580 581
 582 583
 584 585
 586 587
 588 589
 590 591
 592 593
 594 595
 596 597
 598 599
 600 601
 602 603
 604 605
 606 607
 608 609
 610 611
 612 613
 614 615
 616 617
 618 619
 620 621
 622 623
 624 625
 626 627
 628 629
 630 631
 632 633
 634 635
 636 637
 638 639
 640 641
 642 643
 644 645
 646 647
 648 649
 650 651
 652 653
 654 655
 656 657
 658 659
 660 661
 662 663
 664 665
 666 667
 668 669
 670 671
 672 673
 674 675
 676 677
 678 679
 680 681
 682 683
 684 685
 686 687
 688 689
 690 691
 692 693
 694 695
 696 697
 698 699
 700 701
 702 703
 704 705
 706 707
 708 709
 710 711
 712 713
 714 715
 716 717
 718 719
 720 721
 722 723
 724 725
 726 727
 728 729
 730 731
 732 733
 734 735
 736 737
 738 739
 740 741
 742 743
 744 745
 746 747
 748 749
 750 751
 752 753
 754 755
 756 757
 758 759
 760 761
 762 763
 764 765
 766 767
 768 769
 770 771
 772 773
 774 775
 776 777
 778 779
 780 781
 782 783
 784 785
 786 787
 788 789
 790 791
 792 793
 794 795
 796 797
 798 799
 800 801
 802 803
 804 805
 806 807
 808 809
 810 811
 812 813
 814 815
 816 817
 818 819
 820 821
 822 823
 824 825
 826 827
 828 829
 830 831
 832 833
 834 835
 836 837
 838 839
 840 841
 842 843
 844 845
 846 847
 848 849
 850 851
 852 853
 854 855
 856 857
 858 859
 860 861
 862 863
 864 865
 866 867
 868 869
 870 871
 872 873
 874 875
 876 877
 878 879
 880 881
 882 883
 884 885
 886 887
 888 889
 890 891
 892 893
 894 895
 896 897
 898 899
 900 901
 902 903
 904 905
 906 907
 908 909
 910 911
 912 913
 914 915
 916 917
 918 919
 920 921
 922 923
 924 925
 926 927
 928 929
 930 931
 932 933
 934 935
 936 937
 938 939
 940 941
 942 943
 944 945
 946 947
 948 949
 950 951
 952 953
 954 955
 956 957
 958 959
 960 961
 962 963
 964 965
 966 967
 968 969
 970 971
 972 973
 974 975
 976 977
 978 979
 980 981
 982 983
 984 985
 986 987
 988 989
 990 991
 992 993
 994 995
 996 997
 998 999
 1000 1001
 1002 1003
 1004 1005
 1006 1007
 1008 1009
 1010 1011
 1012 1013
 1014 1015
 1016 1017
 1018 1019
 1020 1021
 1022 1023
 1024 1025
 1026 1027
 1028 1029
 1030 1031
 1032 1033
 1034 1035
 1036 1037
 1038 1039
 1040 1041
 1042 1043
 1044 1045
 1046 1047
 1048 1049
 1050 1051
 1052 1053
 1054 1055
 1056 1057
 1058 1059
 1060 1061
 1062 1063
 1064 1065
 1066 1067
 1068 1069
 1070 1071
 1072 1073
 1074 1075
 1076 1077
 1078 1079
 1080 1081
 1082 1083
 1084 1085
 1086 1087
 1088 1089
 1090 1091
 1092 1093
 1094 1095
 1096 1097
 1098 1099
 1100 1101
 1102 1103
 1104 1105
 1106 1107
 1108 1109
 1110 1111
 1112 1113
 1114 1115
 1116 1117
 1118 1119
 1120 1121
 1122 1123
 1124 1125
 1126 1127
 1128 1129
 1130 1131
 1132 1133
 1134 1135
 1136 1137
 1138 1139
 1140 1141
 1142 1143
 1144 1145
 1146 1147
 1148 1149
 1150 1151
 1152 1153
 1154 1155
 1156 1157
 1158 1159
 1160 1161
 1162 1163
 1164 1165
 1166 1167
 1168 1169
 1170 1171
 1172 1173
 1174 1175
 1176 1177
 1178 1179
 1180 1181
 1182 1183
 1184 1185
 1186 1187
 1188 1189
 1190 1191
 1192 1193
 1194 1195
 1196 1197
 1198 1199
 1200 1201
 1202 1203
 1204 1205
 1206 1207
 1208 1209
 1210 1211
 1212 1213
 1214 1215
 1216 1217
 1218 1219
 1220 1221
 1222 1223
 1224 1225
 1226 1227
 1228 1229
 1230 1231
 1232 1233
 1234 1235
 1236 1237
 1238 1239
 1240 1241
 1242 1243
 1244 1245
 1246 1247
 1248 1249
 1250 1251
 1252 1253
 1254 1255
 1256 1257
 1258 1259
 1260 1261
 1262 1263
 1264 1265
 1266 1267
 1268 1269
 1270 1271
 1272 1273
 1274 1275
 1276 1277
 1278 1279
 1280 1281
 1282 1283
 1284 1285
 1286 1287
 1288 1289
 1290 1291
 1292 1293
 1294 1295
 1296 1297
 1298 1299
 1300 1301
 1302 1303
 1304 1305
 1306 1307
 1308 1309
 1310 1311
 1312 1313
 1314 1315
 1316 1317
 1318 1319
 1320 1321
 1322 1323
 1324 1325
 1326 1327
 1328 1329
 1330 1331
 1332 1333
 1334 1335
 1336 1337
 1338 1339
 1340 1341
 1342 1343
 1344 1345
 1346 1347
 1348 1349
 1350 1351
 1352 1353
 1354 1355
 1356 1357
 1358 1359
 1360 1361
 1362 1363
 1364 1365
 1366 1367
 1368 1369
 1370 1371
 1372 1373
 1374 1375
 1376 1377
 1378 1379
 1380 1381
 1382 1383
 1384 1385
 1386 1387
 1388 1389
 1390 1391
 1392 1393
 1394 1395
 1396 1397
 1398 1399
 1400 1401
 1402 1403
 1404 1405
 1406 1407
 1408 1409
 1410 1411
 1412 1413
 1414 1415
 1416 1417
 1418 1419
 1420 1421
 1422 1423
 1424 1425
 1426 1427
 1428 1429
 1430 1431
 1432 1433
 1434 1435
 1436 1437
 1438 1439
 1440 1441
 1442 1443
 1444 1445
 1446 1447
 1448 1449
 1450 1451
 1452 1453
 1454 1455
 1456 1457
 1458 1459
 1460 1461
 1462 1463
 1464 1465
 1466 1467
 1468 1469
 1470 1471
 1472 1473
 1474 1475
 1476 1477
 1478 1479
 1480 1481
 1482 1483
 1484 1485
 1486 1487
 1488 1489
 1490 1491
 1492 1493
 1494 1495
 1496 1497
 1498 1499
 1500 1501
 1502 1503
 1504 1505
 1506 1507
 1508 1509
 1510 1511
 1512 1513
 1514 1515
 1516 1517
 1518 1519
 1520 1521
 1522 1523
 1524 1525
 1526 1527
 1528 1529
 1530 1531
 1532 1533
 1534 1535
 1536 1537
 1538 1539
 1540 1541
 1542 1543
 1544 1545
 1546 1547
 1548 1549
 1550 1551
 1552 1553
 1554 1555
 1556 1557
 1558 1559
 1560 1561
 1562 1563
 1564 1565
 1566 1567
 1568 1569
 1570 1571
 1572 1573
 1574 1575
 1576 1577
 1578 1579
 1580 1581
 1582 1583
 1584 1585
 1586 1587
 1588 1589
 1590 1591
 1592 1593
 1594 1595
 1596 1597
 1598 1599
 1600 1601
 1602 1603
 1604 1605
 1606 1607
 1608 1609
 1610 1611
 1612 1613
 1614 1615
 1616 1617
 1618 1619
 1620 1621
 1622 1623
 1624 1625
 1626 1627
 1628 1629
 1630 1631
 1632 1633
 1634 1635
 1636 1637
 1638 1639
 1640 1641
 1642 1643
 1644 1645
 1646 1647
 1648 1649
 1650 1651
 1652 1653
 1654 1655
 1656 1657
 1658 1659
 1660 1661
 1662 1663
 1664 1665
 1666 1667
 1668 1669
 1670 1671
 1672 1673
 1674 1675
 1676 1677
 1678 1679
 1680 1681
 1682 1683
 1684 1685
 1686 1687
 1688 1689
 1690 1691
 1692 1693
 1694 1695
 1696 1697
 1698 1699
 1700 1701
 1702 1703
 1704 1705
 1706 1707
 1708 1709
 1710 1711
 1712 1713
 1714 1715
 1716 1717
 1718 1719
 1720 1721
 1722 1723
 1724 1725
 1726 1727
 1728 1729
 1730 1731
 1732 1733
 1734 1735
 1736 1737
 1738 1739
 1740 1741
 1742 1743
 1744 1745
 1746 1747
 1748 1749
 1750 1751
 1752 1753
 1754 1755
 1756 1757
 1758 1759
 1760 1761
 1762 1763
 1764 1765
 1766 1767
 1768 1769
 1770 1771
 1772 1773
 1774 1775
 1776 1777
 1778 1779
 1780 1781
 1782 1783
 1784 1785
 1786 1787
 1788 1789
 1790 1791
 1792 1793
 1794 1795
 1796 1797
 1798 1799
 1800 1801
 1802 1803
 1804 1805
 1806 1807
 1808 1809
 1810 1811
 1812 1813
 1814 1815
 1816 1817
 1818 1819
 1820 1821
 1822 1823
 1824 1825
 1826 1827
 1828 1829
 1830 1831
 1832 1833
 1834 1835
 1836 1837
 1838 1839
 1840 1841
 1842 1843
 1844 1845
 1846 1847
 1848 1849
 1850 1851
 1852 1853
 1854 1855
 1856 1857
 1858 1859
 1860 1861
 1862 1863
 1864 1865
 1866 1867
 1868 1869
 1870 1871
 1872 1873
 1874 1875
 1876 1877
 1878 1879
 1880 1881
 1882 1883
 1884 1885
 1886 1887
 1888 1889
 1890 1891
 1892 1893
 1894 1895
 1896 1897
 1898 1899
 1900 1901
 1902 1903
 1904 1905
 1906 1907
 1908 1909
 1910 1911
 1912 1913
 1914 1915
 1916 1917
 1918 1919
 1920 1921
 1922 1923
 1924 1925
 1926 1927
 1928 1929
 1930 1931
 1932 1933
 1934 1935
 1936 1937
 1938 1939
 1940 1941
 1942 1943
 1944 1945
 1946 1947
 1948 1949
 1950 1951
 1952 1953
 1954 1955
 1956 1957
 1958 1959
 1960 1961
 1962 1963
 1964 1965
 1966 1967
 1968 1969
 1970 1971
 1972 1973
 1974 1975
 1976 1977
 1978 1979
 1980 1981
 1982 1983
 1984 1985
 1986 1987
 1988 1989
 1990 1991
 1992 1993
 1994 1995
 1996 1997
 1998 1999
 2000 2001
 2002 2003
 2004 2005
 2006 2007
 2008 2009
 2010 2011
 2012 201

- Carthy, Detection of the aromatic molecule benzonitrile ($c\text{-C}_6\text{H}_5\text{CN}$) in the interstellar medium, *Science* 359 (6372) (2018) 202–205.
- [17] A. Coletta, F. Fontani, V. Rivilla, C. Mininni, L. Colzi, Á. Sánchez-Monge, M. Beltrán, Evolutionary study of complex organic molecules in high-mass star-forming regions, *Astron. Astrophys.* 641 (2020) A54.
- [18] J. K. Jørgensen, A. Belloche, R. T. Garrod, Astrochemistry during the formation of stars, *Ann. Rev. Astron. Astrophys.* 58 (2020) 727–778.
- [19] P. Caselli, T. Hasegawa, E. Herbst, Chemical differentiation between star-forming regions—the orion hot core and compact ridge, *Astrophys. J.* 408 (1993) 548–558.
- [20] S. Spezzano, L. Bizzocchi, P. Caselli, J. Harju, S. Brünken, Chemical differentiation in a prestellar core traces non-uniform illumination, *Astron. Astrophys.* 592 (2016) L11.
- [21] Y. Aikawa, K. Furuya, S. Yamamoto, N. Sakai, Chemical variation among protostellar cores: Dependence on prestellar core conditions, *Astrophys. J.* 897 (2) (2020) 110.
- [22] L. Bizzocchi, F. Tamassia, J. Laas, B. M. Giuliano, C. Degli Esposti, L. Dore, et al., Rotational and high-resolution infrared spectrum of HC_3N : global rovibrational analysis and improved line catalog for astrophysical observations, *Astrophys. J. Suppl. S.* 233 (1) (2017) 11.
- [23] M. Melosso, A. Belloche, M.-A. Martin-Drumel, O. Pirali, F. Tamassia, L. Bizzocchi, et al., Far-infrared laboratory spectroscopy of aminoacetonitrile and first interstellar detection of its vibrationally excited transitions, *Astron. Astrophys.* 641 (2020) A160.
- [24] M. Carvajal, C. Favre, I. Kleiner, C. Ceccarelli, E. Bergin, D. Fedele, Impact of nonconvergence and various approximations of the partition function on the molecular column densities in the interstellar medium, *Astron. Astrophys.* 627 (2019) A65.
- [25] F. Daniel, L. Coudert, A. Punanova, J. Harju, A. Faure, E. Roueff, et al., The NH_2D hyperfine structure revealed by astrophysical observations, *Astron. Astrophys.* 586 (2016) L4.
- [26] J. Harju, F. Daniel, O. Sipilä, P. Caselli, J. E. Pineda, R. K. Friesen, et al., Deuteration of ammonia in the starless core Ophiuchus/H-MM1, *Astron. Astrophys.* 600 (2017) A61.
- [27] M. Melosso, L. Dore, J. Gauss, C. Puzzarini, Deuterium hyperfine splittings in the rotational spectrum of NH_2D as revealed by Lamb-dip spectroscopy, *J. Mol. Spectrosc.* (2020) 111291.
- [28] C. Endres, H. Müller, S. Brünken, D. Paveliev, T. Giesen, S. Schlemmer, F. Lewen, High resolution rotation–inversion spectroscopy on doubly deuterated ammonia, ND_2H , up to 2.6 THz, *J. Mol. Struct.* 795 (1–3) (2006) 242–255.
- [29] M. Melosso, L. Bizzocchi, F. Tamassia, C. Degli Esposti, E. Cané, L. Dore, The rotational spectrum of ^{15}ND : isotopic-independent Dunham-type analysis of the imidogen radical, *Phys. Chem. Chem. Phys.* 21 (2019) 3564–3573.
- [30] M. Melosso, C. Degli Esposti, L. Dore, Terahertz spectroscopy and global analysis of the rotational spectrum of doubly deuterated amidogen radical ND_2 , *Astrophys. J. Suppl. S.* 233 (1) (2017) 15.
- [31] M. Melosso, B. Conversazioni, C. Degli Esposti, L. Dore, E. Cané, F. Tamassia, L. Bizzocchi, The pure rotational spectrum of $^{15}\text{ND}_2$ observed by millimetre and submillimetre-wave spectroscopy, *J. Quant. Spectrosc. Ra.* 222 (2019) 186–189.
- [32] C. Puzzarini, G. Cazzoli, M. E. Harding, J. Vázquez, J. Gauss, A new experimental absolute nuclear magnetic shielding scale for oxygen based on the rotational hyperfine structure of H^{17}_2O , *J. Chem. Phys.* 131 (2009) 234304.
- [33] C. Puzzarini, G. Cazzoli, M. E. Harding, J. Vázquez, J. Gauss, The hyperfine structure in the rotational spectra of D^{17}_2O and HD^{17}O : Confirmation of the absolute nuclear magnetic shielding scale for oxygen, *J. Chem. Phys.* 142 (2015) 124308.
- [34] L. Dore, L. Bizzocchi, C. Degli Esposti, J. Gauss, The magnetic hyperfine structure in the rotational spectrum of H_2CNH , *J. Mol. Spectrosc.* 263 (2010) 44–50.
- [35] L. Bizzocchi, M. Melosso, B. M. Giuliano, L. Dore, F. Tamassia, M.-A. Martin-Drumel, et al., Submillimeter and far-infrared spectroscopy of monodeuterated amidogen radical (NHD): Improved rest frequencies for astrophysical observations, *Astrophys. J. Suppl. S.* 247 (2) (2020) 59.
- [36] M. Melosso, L. Bizzocchi, A. Adamczyk, E. Cané, P. Caselli, L. Colzi, et al., Extensive ro-vibrational analysis of deuterated-cyanoacetylene (DC_3N) from millimeter-wavelengths to the infrared domain, *J. Quant. Spectrosc. Ra.* 254 (2020) 107221.
- [37] H. S. Müller, F. Schlöder, J. Stutzki, G. Winnewisser, The cologne database for molecular spectroscopy, CDMS: a useful tool for astronomers and spectroscopists, *J. Mol. Struct.* 742 (1–3) (2005) 215–227.
- [38] K. Raghavachari, G. W. Trucks, J. A. Pople, M. Head-Gordon, A fifth-order perturbation comparison of electron correlation theories, *Chem. Phys. Lett.* 157 (1989) 479–483.
- [39] T. H. Dunning Jr., Gaussian Basis Sets for Use in Correlated Molecular Calculations. I. The Atoms Boron through Neon and Hydrogen, *J. Chem. Phys.* 90 (1989) 1007.
- [40] A. Kendall, T. H. Dunning Jr., R. J. Harrison, Electron affinities of the first-row atoms revisited. Systematic basis sets and wave functions, *J. Chem. Phys.* 96 (1992) 6796.
- [41] D. E. Woon, T. H. Dunning Jr., Gaussian basis sets for use in correlated molecular calculations. V. Core-valence basis sets for boron through neon, *J. Chem. Phys.* 103 (1995) 4572.
- [42] A. K. Wilson, T. van Mourik, T. H. Dunning Jr, Gaussian basis sets for use in correlated molecular calculations. VI. Sextuple zeta correlation consistent basis sets for boron through neon, *J. Mol. Struct. THEOCHEM* 388 (1996) 339–349.
- [43] T. Van Mourik, A. K. Wilson, T. H. Dunning Jr, Benchmark calculations with correlated molecular wavefunctions. XIII. Potential energy curves for He_2 , Ne_2 and Ar_2 using correlation consistent basis sets through augmented sextuple zeta, *Mol. Phys.* 96 (1999) 529–547.
- [44] C. Puzzarini, M. Heckert, J. Gauss, The accuracy of rotational constants predicted by high-level quantum-chemical calculations. i. molecules containing first-row atoms, *J. Chem. Phys.* 128 (19) (2008) 194108.
- [45] I. M. Mills, Vibration-rotation structure in asymmetric and symmetric-top molecules, Vol. 1, 1972, p. 115.
- [46] J. F. Stanton, J. Gauss, L. Cheng, M. E. Harding, D. A. Matthews, P. G. Szalay, CFOUR, coupled-cluster

- 633 techniques for computational chemistry, a quantum- 698
634 chemical program package, With contributions from 699
635 A.A. Auer, R.J. Bartlett, U. Benedikt, C. Berger, 700
636 D.E. Bernholdt, Y.J. Bomble, O. Christiansen, F. En- 701
637 gel, R. Faber, M. Heckert, O. Heun, M. Hilgenberg, 702
638 C. Huber, T.-C. Jagau, D. Jonsson, J. Jusélius, T. 703
639 Kirsch, K. Klein, W.J. Lauderdale, F. Lipparini, T.
640 Metzroth, L.A. Mück, D.P. O'Neill, D.R. Price, E.
641 Prochnow, C. Puzzarini, K. Ruud, F. Schiffmann, W.
642 Schwalbach, C. Simmons, S. Stopkowicz, A. Tajti, J.
643 Vázquez, F. Wang, J.D. Watts and the integral pack-
644 ages MOLECULE (J. Almlöf and P.R. Taylor), PROPS
645 (P.R. Taylor), ABACUS (T. Helgaker, H.J. Aa. Jensen,
646 P. Jørgensen, and J. Olsen), and ECP routines by A.
647 V. Mitin and C. van Wüllen. For the current version,
648 see <http://www.cfour.de>.
- [47] D. A. Matthews, L. Cheng, M. E. Harding, F. Lipparini,
649 S. Stopkowicz, T.-C. Jagau, et al., Coupled-cluster tech-
650 niques for computational chemistry: The cfour program
651 package, *J. Chem. Phys.* 152 (21) (2020) 214108.
- [48] M. Kállay, MRCC, a generalized CC/CI program, For
652 the current version, see <http://www.mrcc.hu>.
- [49] M. Kállay, P. R. Nagy, D. Mester, Z. Rolik, G. Samu,
653 J. Csontos, et al., The mrcc program system: Accurate
654 quantum chemistry from water to proteins, *J. Chem.*
655 *Phys.* 152 (7) (2020) 074107.
- [50] T. Helgaker, J. Gauss, G. Cazzoli, C. Puzzarini, ^{33}S
656 hyperfine interactions in H_2S and SO_2 and revision of
657 the sulfur nuclear magnetic shielding scale, *J. Chem.*
658 *Phys.* 139 (2013) 244308.
- [51] M. Weiss, M. W. P. Strandberg, The microwave spectra
659 of the deuterio-ammonias, *Phys. Rev.* 83 (1951) 567.
- [52] M. Lichtenstein, J. Gallagher, V. Derr, Spectroscopic
660 investigations of the deuterio-ammonias in the millime-
661 ter region, *J. Mol. Spectrosc.* 12 (1) (1964) 87–97.
- [53] F. C. De Lucia, P. Helminger, Millimeter-and
662 submillimeter-wave length spectrum of the partially
663 deuterated ammonias; a study of inversion, centrifugal
664 distortion, and rotation-inversion interactions, *J. Mol.*
665 *Spectrosc.* 54 (1975) 200–214.
- [54] E. Cohen, H. Pickett, The rotation-inversion spectra
666 and vibration-rotation interaction in NH_2D , *J. Mol.*
667 *Spectrosc.* 93 (1982) 83–100.
- [55] L. Fusina, G. Di Lonardo, J. Johns, L. Halonen, Far-
668 infrared spectra and spectroscopic parameters of NH_2D
669 and ND_2H in the ground state, *J. Mol. Spectrosc.* 127
670 (1988) 240–254.
- [56] H. M. Pickett, The fitting and prediction of vibration-
671 rotation spectra with spin interactions, *J. Mol. Spec-*
672 *trosc.* 148 (1991) 371–377.
- [57] M. Tafalla, P. Myers, P. Caselli, C. Walmsley,
673 C. Comito, Systematic molecular differentiation in star-
674 less cores, *Astrophys. J.* 569 (2) (2002) 815.
- [58] E. Keto, P. Caselli, Dynamics and depletion in ther-
675 mally supercritical starless cores, *Mon. Not. R. Astron.*
676 *Soc.* 402 (3) (2010) 1625–1634.
- [59] E. Redaelli, L. Bizzocchi, P. Caselli, O. Sipilä, V. Lat-
677 tanzi, B. Giuliano, S. Spezzano, High-sensitivity maps
678 of molecular ions in l1544-i. deuteration of $\text{n}2\text{h}^+$ and
679 hco^+ and primary evidence of $\text{n}2\text{d}^+$ depletion, *Astron.*
680 *Astrophys.* 629 (2019) A15.
- [60] S. Spezzano, S. Brünken, P. Schilke, P. Caselli,
681 K. Menten, M. McCarthy, et al., Interstellar detection
682 of $\text{c-C}_3\text{D}_2$, *Astrophys. J. Lett.* 769 (2) (2013) L19.
- [61] S. Spezzano, H. Gupta, S. Brünken, C. Gottlieb,
683 P. Caselli, K. Menten, et al., A study of the C_3H_2 iso-
684 mers and isotopologues: first interstellar detection of
685 HDCCC, *Astron. Astrophys.* 586 (2016) A110.
- [62] L. Bizzocchi, P. Caselli, S. Spezzano, E. Leonardo,
686 Deuterated methanol in the pre-stellar core L1544, *As-*
687 *tron. Astrophys.* 569 (2014) A27.